Sensors and Actuators B 150 (2010) 19–24

Contents lists available at ScienceDirect

Sensors and Actuators B: Chemical

journal homepage: www.elsevier.com/locate/snb

Room temperature CO gas sensing using Zn-doped In_2O_3 single nanowire field effect transistors

Nandan Singh, Chaoyi Yan, Pooi See Lee*

School of Materials Science and Engineering, Nanyang Technological University, 50 Nanyang Avenue 639798, Singapore

ARTICLE INFO

Article history:
Received 26 April 2010
Received in revised form 26 July 2010
Accepted 28 July 2010
Available online 5 August 2010

Keywords:
Zn-doped In_2O_3
NW-FET
Doping
Sensing
Sensor response

ABSTRACT

We demonstrate a room temperature sensing of CO gas (1–5 ppm) using high performance single Zn-doped In_2O_3 nanowire field effect transistors (Zn–In_2O_3 NW-FETs). Zn–In_2O_3 nanowires were grown in a horizontal CVD furnace; single Zn–In_2O_3 NW-FETs were fabricated using SiN_x dielectric layer and bottom gate. Electrical measurements on the NW-FETs showed high performance devices, with a high "ON" current of 8×10^{-6} A at a 5 V drain voltage, high on-off ratio of $\sim 10^6$ and electron mobility of 139 $cm^2 V^{-1} s^{-1}$. Sensing properties of CO gas were studied using these NW-FETs at room temperature. Doping of Zn^{2+} into the In_2O_3 NW enhances the sensor response compared to pure In_2O_3 nanowire. A good selectivity of CO gas over NO and NO_2 can also be achieved. The improved sensor response at room temperature is attributed to the defects created and a change in conductivity of the nanowire upon Zn-doping. Significant negative threshold voltage shift of −3.5 V was observed after exposure to a low concentration of CO gas at 5 ppm. This approach represents an important step towards the room temperature sensing of hazardous gas.

1. Introduction

Among the sensing materials, oxides are widely used in the electrical detection of the pollutant gases due to their ability to change the conductivity when it comes in contact to the gas molecules. Semiconductor oxides such as In_2O_3 [1–3], ZnO [4,5], SnO_2 [6], etc. are well explored for pollutant gases sensor. In order to increase the sensitivity, nanomaterials with higher surface area are advantageous [7]. There are various kind of nanostructures that have been used as sensors, including nanoparticles [8], nanowires [9–12], nanotubes [13], nanobelts [14], nanosheets [15], and nanocubes [16]. Single one-dimensional (1D) nanostructure based devices have attracted much attention due to their great miniaturization potential and large surface to volume ratio at nanoscale level which allows quick diffusion of gas molecules. As a result higher sensitivity and low detection limit with fast response and recovery time can be achieved even at lower working temperature range.

In room temperature operation, most of the gas sensors still face difficulties in getting a high response. Some reports have shown possible room temperature operation with higher sensitivity for NO_2 using In_2O_3 nanowires [3]. In order to attain high response and selectivity, different approaches such as microstructure control, doping, raising operating temperature, etc. have been adopted to modify the sensing properties of semiconductor metal oxide gas sensors [17,18]. It is well known that the sensing mechanism is based on the surface reaction of the nanostructure with the exposed gas (adsorption and desorption of the test gas molecules). As adsorption is a surface effect, one can increase the adsorption of gas molecules by decorating with nanoparticles or doping with an element which has a stronger chemical affinity for that particular gas molecule. Doping in the nanowire can create defects and these defects play a role as preferential adsorption sites for gas molecule which can help to sense pollutant gases at lower temperature [19].

Carbon monoxide (CO) gas is one of the major pollutant gases in the environment and is mostly produced by the automobiles and industrial processes. It adversely affects human health at only a few parts per million. In most of the cases the CO gas detection sensitivity has been limited to 4–10 ppm with low response even at higher temperature [20,21]. Recently, Aruna et al. [22] have reported the ppb level detection of CO gas using SnO_x-Pb nanoparticles at 350 °C and Joshi et al. [4] have reported a room temperature detection of 100 ppm CO gas using Au decorated ZnO NWs. There is no report on the detection of sub 10 ppm CO gas at room temperature in the best of our knowledge. The aim of this work is to overcome the requirement of high operation temperature for CO gas sensing of high sensitivity using nanowire field effect transistors. Here we report on the effect of Zn-doping on the sensing of CO gas at room temperature using high performance In_2O_3 NW-FETs.

* Corresponding author. Tel.: +65 6790 6661; fax: +65 6790 9081.
E-mail address: pslee@ntu.edu.sg (P.S. Lee).

0925-4005/$ – see front matter © 2010 Elsevier B.V. All rights reserved.
doi:10.1016/j.snb.2010.07.051

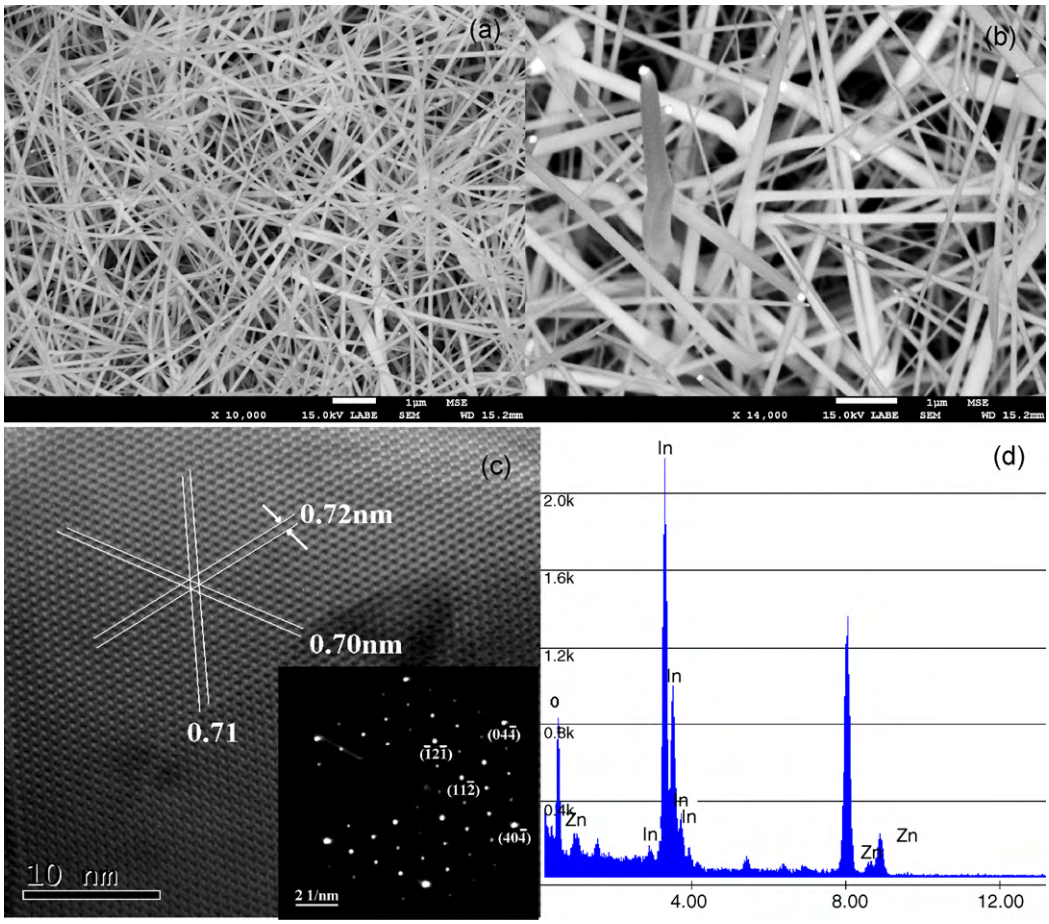

Fig. 1. (a and b) FESEM images of the as-grown Zn–In_2O_3 NW under low and high magnification, the images were captured in the low angle back scattered electron detection (LABE) mode, (c) HRTEM image of the Zn–In_2O_3 NW, showing a family of {1 1 0} planes with inter planar distance 0.71 nm and in the inset SAD pattern is indexed and taken along [1 1 1] zone axis, (d) EDS pattern measured on a single Zn–In_2O_3 NW, showing a series of In, O and weak Zn peaks.

2. Experimental work

Zn–In_2O_3 NWs were grown in a horizontal CVD furnace at a source temperature of 900 °C [23]. The source for the growth was taken as a mixture of ZnO and In_2O_3 with graphite powder. During the deposition, argon gas flow rate was fixed at 50 sccm and the pressure inside the quartz tube was maintained at 1 mbar. Si substrates with 9 nm gold layer were kept downstream and the substrate temperature ranges from 400 to 550 °C with deposition duration of 60 min. The as-grown Zn–In_2O_3 samples were then annealed at 600 °C for 4 h in atmosphere.

The morphology of the as-grown samples was studied by field emission scanning electron microscopy (FESEM) on a JEOL 7600F scanning electron microscope operated at 5 kV. High resolution transmission electron micrographs (HRTEM) and selected-area diffraction (SAD) patterns were collected using a JEOL JEM 2010 microscope at an accelerating voltage of 200 kV. Energy-dispersive X-ray spectroscopy (EDS) analysis of a single nanowire was done on a JEOL JEM 2100F microscope. Photoluminescence studies were carried out at room temperature on a Cary Eclipse EL system at an excitation wavelength of 264 nm.

Zn–In_2O_3 nanowire-based devices were fabricated on a highly doped n-type silicon wafer with a 60 nm SiN_x high-k dielectric layer. Standard optical-lithography followed by Cr/Au (10/50 nm) deposition and liftoff was used to define the contact electrodes. The highly conductive Si substrate (resistivity 0.005 Ω cm) was used as a global back gate. Isopropyl alcohol (IPA) solution containing Zn–In_2O_3 nanowires was prepared and drop-casted onto the Si substrate. After drying, locations of nanowires on the pads (electrodes) were identified for fabricating nanowire-based field effect transistor (FET) structures. All the electrical and sensing measurements on the nanowire FET were done on a Keithley 4200-SCS semiconductor characterization system, attached with an optical microscope and sensing gases with gas controller under a humidity level of 50% at room temperature.

The sensor response (S %) is defined as, $S\% = [|\Delta R|/R_0] \times 100$, where ΔR is the difference in resistances before and after gas exposure which is an absolute value, and R_0 is the initial resistance of the nanowire sensor.

3. Result and discussion

The morphology of the as-grown Zn–In_2O_3 NWs is shown in Fig. 1(a) and (b). The presence of the Au catalyst at the nanowire tip indicates the vapor–liquid–solid (VLS) nanowire growth mechanism. As shown in the FESEM images, the as-grown nanowires have a diameter of 50–300 nm and a length of 10–30 μm with circular cross-section. Fig. 1(c) shows a HRTEM image of the nanowire with an interplanar distance of 0.70 nm for {1 1 0} when viewing along ⟨1 1 1⟩. The SAD (in the inset of Fig. 1(c)) pattern was taken along [1 1 1] zone axis and indexed accordingly, which reveals that the nanowire has single crystalline cubic structure. In Fig. 1(d), the EDS pattern measured on a single Zn–In_2O_3 NW showed a weak Zn peak with 1.6 at% Zn inclusion in the In_2O_3 NW. It has been reported that the solubility of Zn in the In_2O_3 lattice is low [22], which agrees well with our result. In addition, we have observed a

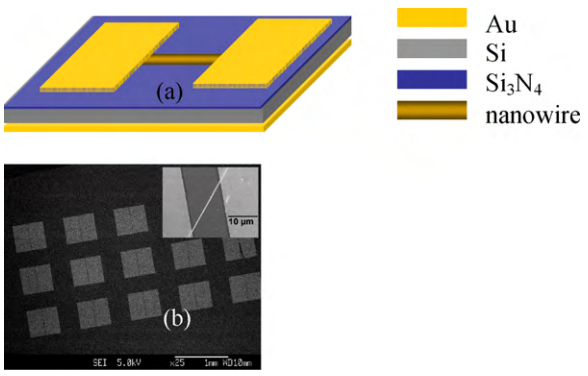

Fig. 2. (a) Schematic diagram of single nanowire FET, with Cr (10 nm)\Au (50 nm) serving as electrodes, SiN_x serving as gate electrode and highly doped (resistivity 0.005 Ω cm) n-type Si as back gate, (b) FESEM image of a array of devices and in the inset a single NW-FET device touching the two electrodes with a channel length of 18 μm.

shift in the XRD peaks (supporting information S1) towards higher theta value, which confirms the presence of Zn in the In_2O_3 lattice.

Fig. 2(a) shows a schematic illustration of a transistor based electrical sensor. Nanowires (with 1.6 at% Zn) were dispersed on a 60 nm SiN_x high-k dielectric layer on Si substrate with patterned source and drain electrodes. The highly doped n-type Si substrate served as a back gate electrode and the chemical sensor was realized using this FET based sensor. Fig. 2(b) shows a representative FESEM image of the single Zn–In_2O_3 NW bridging between two electrodes with a channel length of 18 μm. Similar nanowire transistors were fabricated using the undoped In_2O_3 NWs.

It is important and advantageous to realize highly functional NW-FET devices for the purpose of optimized sensing properties. It has been reported that Zn–In_2O_3 NW-FET shows a remarkable n-type FET characteristics [22,24]. The transport properties of our single NW-FET device exhibited excellent n-type characteristics with strong gate control. The family curves for current–voltage (I_d–V_d) characteristics measured on a single nanowire as shown in Fig. 3(a), indicates a good conductivity of the nanowire with a high "ON" state current of 8×10^{-6} A at 5 V drain voltage (V_d). Fig. 3(b) shows the I_d–V_g curve recorded from the same device at $V_d = 5$ V, with a linear behavior above a threshold voltage V_T of −15.65 V. A sub-threshold swing value of ~140 mV/decade and a drain–source current on/off ratio ~1×10^6 can be achieved, which are comparable to one of the best reported values [22]. The electron mobility (μ_e) was determined to be 139 $cm^2\,V^{-1}\,s^{-1}$ in the linear operation region using the equation $\mu = (1/C)[g_m](L^2/V_d)$ [21]; where, g_m is the transconductance (2.216 μS), L is the nanowire channel length (18 μm) and $C = 2\pi\varepsilon\varepsilon_o L/\cosh^{-1}(1 + h/r)$ is the approximate nanowire capacitance; where ε is the dielectric constant of Si_3N_4 (~7), h is the thickness of the Si_3N_4 layer (60 nm), and r is the radius of the nanowire (125 nm). For the undoped single In_2O_3 NW-FET a threshold voltage of −21.5 V, an "ON" state current of 8.5×10^{-6} A with an on/off current ratio of 5×10^5 was measured at 5 V drain voltage.

The Zn–In_2O_3 NW-FET sensors were used for the detection of pollutant gas carbon monoxide (CO) at room temperature. The system was purged with N_2 gas to remove the excessive oxygen species from the surface of the nanowire and chamber. There was a slight current increment during the N_2 purge due to the partial desorption of the ionized oxygen species from the nanowire surface. Drain voltage (V_d) was kept constant at 3 V and gate voltage (V_g) was kept constant at −15 V (which is in the threshold region of the NW-FET) during the measurements. The response of the Zn–In_2O_3 NW sensor for 1–5 ppm CO gas is shown in Fig. 4(a). The change in the current for 1 ppm CO gas was not as significant as for 2 ppm and above (Fig. 4(a)). We can detect distinct electrical changes for the CO gas concentration down to 2 ppm using these Zn–In_2O_3 NW sensors at room temperature. An increase in sensing current can be observed during CO gas exposure (Fig. 4(b)). As shown in Fig. 4(c), the sensor response plot of the Zn–In_2O_3 NW sensor for 5 ppm CO gas shows a response time of 20 s and recovery time of 10 s, this is superior compared to the response time of the undoped In_2O_3 NWs (Fig. 4(d)).

To further probe the selectivity of the Zn–In_2O_3 NW sensor, we have measured the response of the same sensor to other pollutant gases including NO and NO_2 under the same conditions of drain bias voltage of 3 V and gate voltage $V_g = -15$ V. The response of the Zn–In_2O_3 NW sensor compared to different gases is shown in Fig. 5. It is evidently shown that the Zn-doped NW sensors attained a good selectivity of CO gas over NO and NO_2 at room temperature, despite a moderate response (30%) for 2 ppm NO_2 (which is considered as a highly oxidizing gas and has a threshold limit in sub ppb range). A negative threshold voltage (V_T) shift of ~3.5 V was measured after 5 ppm CO gas exposure at room temperature. This negative shift in threshold voltage can be explained in terms of the change in carrier concentration. After exposure to CO gas one can expect an increase in the electrons concentration in an n-type semiconductor. As CO gas molecules react with the ionized oxygen species and form CO_2, electrons are released into the nanowire ($CO + O^- \rightarrow CO_2 + e^-$). This can lead to a negative shift in the threshold voltage after exposure to CO gas due to the increased electrons concentration.

To understand the effect of Zn-doping in CO sensing, 5 ppm CO gas was tested at room temperature using both Zn-doped and undoped In_2O_3 NWs. The response of the Zn–In_2O_3 NW sensor was found to be almost 3 times higher than the undoped nanowire sensor with fast response and recovery time (Fig. 4(d)). The response and recovery time for the Zn–In_2O_3 NWs sensor was found to be

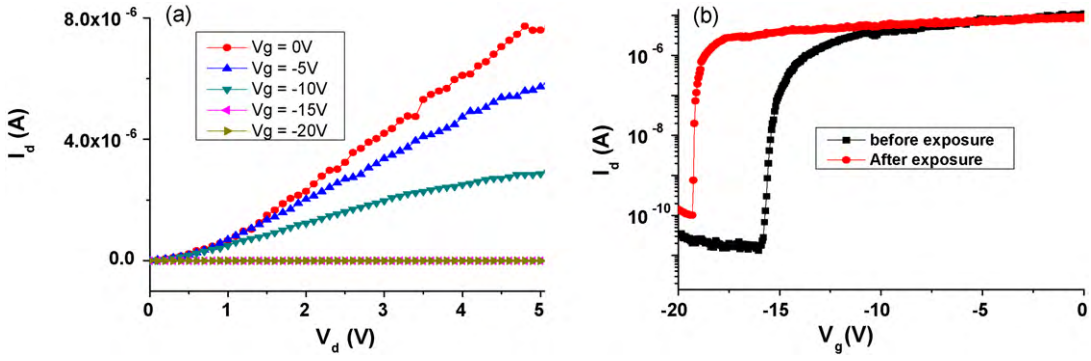

Fig. 3. Electrical measurements done on the single NW-FET: (a) family of drain current–voltage (I_d–V_d) characteristics at different gate voltage (V_g), (b) I_d–V_g curve before and after 5 ppm CO gas exposure, showing a negative threshold voltage shift after exposure to CO gas for 1500 s.

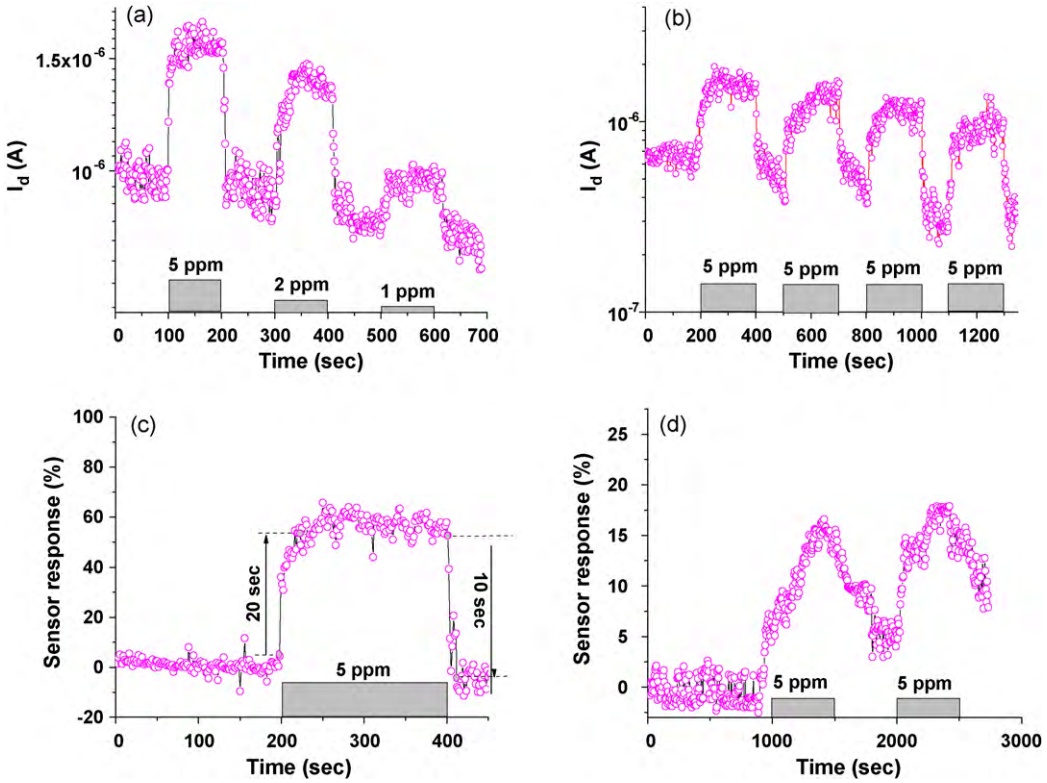

Fig. 4. Gas testing plots for sensor operated at room temperature: (a) I_d–time plot for the Zn–In_2O_3 NW sensor at different CO gas concentrations, (b) I_d–time plot measured on the Zn–In_2O_3 NW sensor when exposed to 5 ppm CO gas in different cycles, (c) sensor response plot of the Zn–In_2O_3 NW sensor for single cycle of 5 ppm CO gas, showing a response time of 20 s and recovery time of 10 s, (d) response plot for the undoped In_2O_3 NW-FET, when exposed to 5 ppm CO gas in two cycles. The drain and gate voltages were kept constant at $V_d = 3$ V and $V_g = -15$ V, respectively, in all sensing experiments.

consistently improved, which shows that doping is playing a crucial role in enhancing the sensor response towards CO gas at room temperature. In addition to the nanowire properties, maintaining gate voltage (V_g) near the threshold region while sensing is important as the devices are very sensitive to the change in carrier concentration at this voltage range and results in a quick response.

3.1. Sensing mechanism

The main effects of doping in oxide semiconducting nanowires are the change in electronic conductivity and the introduction of defects into the nanowires. These factors play an important role to enhance the sensitivity in nanowire sensors. Defects within the crystal structure can improve the adsorption of gas molecules on the nanowire surface [19] and the change in the conductivity will change the position of Fermi level in the energy band diagram which governs the electronic transportation between gas molecule and nanowire material. In addition, the electrical detection of any chemical species is dependent on the surface reactions between the nanowires and the chemical molecules. Since the amount of Zn insertion into the nanowires was found to be small (~1.6 at%), it is unlikely that solely chemical affinity between Zn and CO can lead to the significant CO gas detection enhancement.

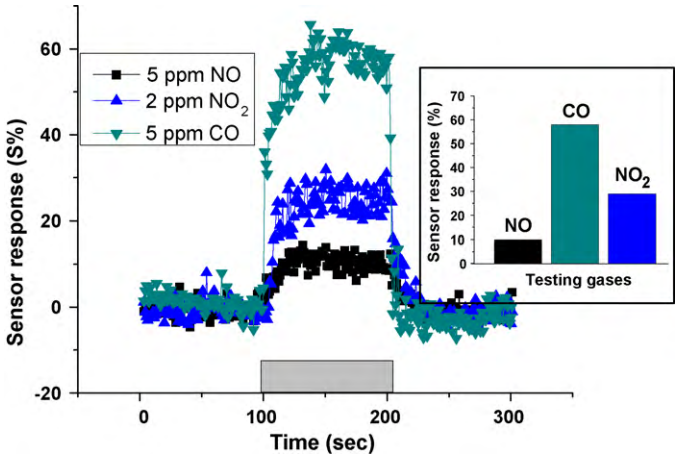

Fig. 5. Response of single Zn–In_2O_3 NW sensor to the different gases at a fixed $V_d = 3$ V and $V_g = -15$ V, sensor was operated at room temperature.

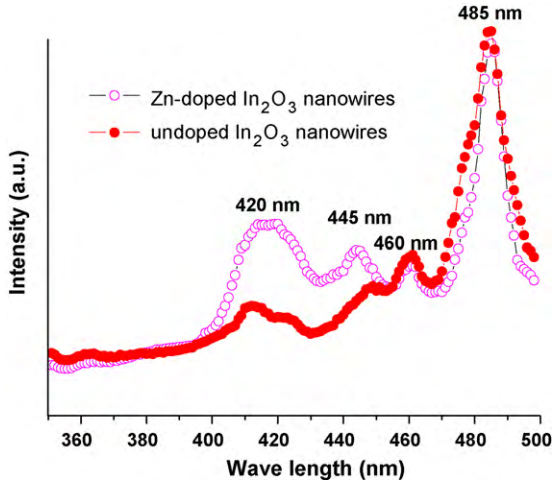

Fig. 6. Photoluminescence spectrum measured from the as deposited Zn-doped and -undoped In_2O_3 NWs with an excitation wavelength of 264 nm at room temperature.

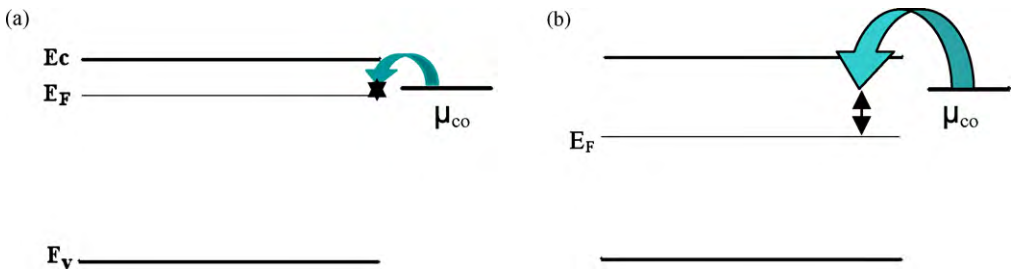

Fig. 7. Energy band diagram of (a) undoped In_2O_3, a n-type semiconductor, (b) Zn–In_2O_3, a less n-type semiconductor with EF moved slightly towards E_v compared to undoped In_2O_3. μ_{co} represents the chemical potentials of the CO molecule.

A plausible explanation on the improved sensing behavior in the doped semiconductor compared to undoped nanowires is related to the defects created by doping. Doping in nanowires can generate defects such as oxygen vacancies, metal interstitials, surface defects, etc. [25,26] and these defects play a vital role in the sensing of CO gas. The defects generated can be evaluated based on the PL spectrum (shown in Fig. 6) taken from the Zn-doped and undoped In_2O_3 NWs under the excited wavelength of 264 nm of a Xe lamp. A series of PL peaks (420 nm, 445 nm, 460 nm and 485 nm) belonging to different types of defects [25,26] can be found. Additional PL peaks (420 nm and 445 nm) have been observed from the Zn-doped sample. These extra peaks can be attributed to the neutral and ionized oxygen vacancies (V_o, $V_o^{\cdot}$ and $V_o^{\cdot\cdot}$) and metal vacancies ($V_{In}^{'''}$) created by Zn-doping at high processing temperature [25]. At this stage we could not assign these PL peaks to the specific kind of defects, because a clear understanding on the photoluminescence behavior and its origin has not been achieved despite a huge number of reports. Most of the defects can play a role of as the preferential adsorption site for a gas molecule [19]. We suggest that this promotes the activation of doped nanowires even at room temperature when reacting with the testing gas.

Electronic transport between nanowire and CO gas molecule can be explained in terms of the transfer of electrons from CO gas molecule to the nanowire due to the chemical potential gradient between semiconducting In_2O_3 nanowire and CO molecule [17]. It is well known that as-grown In_2O_3 behaves as n-type semiconductor due to the existence of the native defects (metal interstitials, oxygen vacancies) in it. In the energy band diagram, the resultant position of E_F is nearer to E_C for undoped In_2O_3 (shown in Fig. 7(a)) where E_C, E_v and E_F correspond to the conduction band, the valence band and the Fermi level of the In_2O_3 NWs. After Zn-doping, there is a slight increase (due to the low 1.6 at% Zn insertion) in the resistance (supporting information S2) but overall the nature of the Zn–In_2O_3 NW still remains n-type. In the band diagram for Zn–In_2O_3 NW, E_F can be slightly shifted towards E_v (Fig. 7(b)) compared to undoped In_2O_3 band diagram (Fig. 7(a)). A chemical potential level μ_{co}, is drawn for CO to represent the chemical potential of the electrons present in the gas molecule that can participate in the electron transfer process. An electron depletion region exists near the surface of the metal oxide nanowires because of the oxygen adsorption on the nanowire surface which extracts electrons from the nanowire, resulting in lower concentration of electrons near the nanowire surface. When CO molecules adsorb onto the In_2O_3 NW surface, electrons transfer starts from a higher chemical potential to the material with a lower chemical potential until the system reaches equilibrium. For the undoped In_2O_3 NW there is a smaller chemical potential gradient between the adsorbed CO molecule and the undoped In_2O_3 compared to the Zn–In_2O_3. This results in the lesser electron transfer (to reach equilibrium) and therefore slower sensor response output with lower sensitivity for the undoped In_2O_3 NWs. On the other hand, the larger difference in the chemical potential of the CO molecule and Zn–In_2O_3 NW gives us faster (response time 20 s and recovery time 10 s) and larger transfer of electrons, hence better sensor response can be achieved.

4. Conclusions

We have developed a strategy to realize room temperature gas sensing using high quality Zn–In_2O_3 NW channel in NW-FETs. The as fabricated device showed excellent operating characteristics with a high drain current on/off modulation ratio of 10^6, a high on-state current of 8×10^{-6} A at $V_d = 5$ V, a small sub-threshold gate voltage swing of 140 mV/decade and an electron mobility of 139 $cm^2\ V^{-1}\ s^{-1}$. Gas sensing properties of such sensor has been studied for 1–5 ppm CO gas at room temperature. A negative threshold voltage shift of −3.5 V was observed after exposure to 5 ppm CO gas. An enhanced sensor response and a good selectivity over NO and NO_2 were achieved which have been correlated to the defects generated and the modification of the Fermi level in a Zn–In_2O_3 NW due to the Zn-doping.

Acknowledgements

The authors gratefully acknowledge Prof. E. Comini and Dr. J. Yan for the insightful discussion and D. Fam, W. Ye for the technical support. N. Singh and C. Yan acknowledge the research scholarship provided by Nanyang Technological University, Singapore.

Appendix A. Supplementary data

Supplementary data associated with this article can be found, in the online version, at doi:10.1016/j.snb.2010.07.051.

References

[1] P. Xu, Z. Cheng, Q. Pan, J. Xu, Q. Xiang, W. Yu, Y. Chu, High aspect ratio In_2O_3 nanowires: synthesis, mechanism and NO_2 gas-sensing properties, Sens. Actuat. B: Chem. 130 (2008) 802–808.
[2] E. Comini, G. Faglia, M. Ferroni, G. Sberveglieri, Controlled growth and sensing properties of In_2O_3 nanowires, Cryst. Growth Des. 7 (2007) 2500–2504.
[3] D.H. Zhang, Z.Q. Liu, C. Li, T. Tang, X.L. Liu, S. Han, B. Lei, C.W. Zhou, Detection of NO_2 down to ppb levels using individual and multiple In_2O_3 nanowire devices, Nano Lett. 4 (2004) 1919–1924.
[4] R.K. Joshi, Q. Hu, F. Alvi, N. Joshi, A. Kumar, Au decorated zinc oxide nanowires for CO sensing, J. Phys. Chem. C 113 (2009) 16199–16202.
[5] C.Y. Liu, C.F. Chen, J.P. Leu, Fabrication and CO sensing properties of mesostructured ZnO gas sensors, J. Elec. Chem. Soc. 156 (1) (2009) 16–19.
[6] I. Aruna, F.E. Kruis, S. Kundu, M. Muhler, R. Theissmann, M. Spasova, CO ppb sensors based on monodispersed SnO_x:Pd mixed nanoparticle layers: insight into dual conductance response, J. Appl. Phys. 105 (2009), 064312/1–064312/8.
[7] X.J. Huang, Y.K. Choi, Chemical sensors based on nanostructured materials, Sens. Actuat. B: Chem. 122 (2007) 659–671.
[8] K. Soulantica, L. Erades, M. Sauvan, F. Senocq, A. Maisonnat, B. Chaudret, Synthesis of indium and indium oxide nanoparticles from indium cyclopentadienyl precursor and their application for gas sensing, Adv. Funct. Mater. 13 (2003) 553–557.
[9] J.H. Park, J.H. Lee, Gas sensing characteristics of polycrystalline SnO_2 nanowires prepared by polyol method, Sens. Actuat. B: Chem. 136 (2009) 151–157.

[10] Y.J. Choi, I.S. Hwang, J.G. Park, K.J. Choi, J.H. Park, J.H. Lee, Novel fabrication of an SnO_2 nanowire gas sensor with high sensitivity, Nanotechnology 19 (2008), 095508/1–095508/4.
[11] Z. Liu, T. Yamazaki, Y. Shen, T. Kikuta, N. Nakatani, Y. Li, O_2 and CO sensing of Ga_2O_3 multiple nanowire gas sensors, Sens. Actuat. B: Chem. 129 (2008) 666–670.
[12] I.S. Hwang, Y.S. Kim, S.J. Kim, B.K. Ju, J.H. Lee, A facile fabrication of semiconductor nanowires gas sensor using PDMS patterning and solution deposition, Sens. Actuat. B: Chem. 136 (2009) 224–229.
[13] O.K. Varghese, D. Gong, M. Paulose, K.G. Ong, E.C. Dickey, C.A. Grimes, Extreme changes in the electrical resistance of titania nanotubes with hydrogen exposure, Adv. Mater. 15 (2003) 624–627.
[14] E. Comini, G. Faglia, G. Sberveglieri, Z. Pan, Z.L. Wang, Stable and highly sensitivegas sensors based on semiconducting oxide nanobelts, Appl. Phys. Lett. 81 (2002) 1869–1871.
[15] C.S. Moon, H.R. Kim, G. Auchterlonie, J. Drennan, J.H. Lee, Highly sensitive and fast responding CO sensor using SnO_2 nanosheets, Sens. Actuat. B: Chem. 131 (2008) 556–564.
[16] C. Xiangfeng, J. Dongli, Z. Chenmou, The preparation and gas-sensing properties of $NiFe_2O_4$ nanocubes and nanorods, Sens. Actuat. B: Chem. 123 (2007) 793–797.
[17] D.H. Zhang, C. Li, X.L. Liu, S. Han, T. Tang, C.W. Zhou, Doping dependent NH_3 sensing of indium oxide nanowires, Appl. Phys. Lett. 83 (2003) 1845–1847.
[18] C. Li, D.H. Zhang, B. Lei, S. Han, X.L. Liu, C.W. Zhou, Surface treatment and doping dependence of In_2O_3 nanowires as ammonia sensors, J. Phys. Chem. B 107 (2003) 12451–12455.
[19] M.W. Ahn, K.S. Park, J.H. Heo, J.G. Park, D.W. Kim, K.J. Choi, J.H. Lee, S.H. Hong, Gas sensing properties of defect controlled ZnO-nanowire gas sensor, Appl. Phys. Lett. 93 (2008), 263103/1–263103/3.
[20] G. Zhang, M.L. Liu, Effect of particle size and dopant on properties of SnO_2-based gas sensors, Sens. Actuat. B: Chem. 69 (2000) 144–152.
[21] L. Liao, Z. Zhang, B. Yan, Z. Zheng, Q.L. Bao, T. Wu, C.M. Li, Z.X. Shen, J.X. Zhang, H. Gong, J.C. Li, T. Yu, Multifunctional CuO nanowire devices: p-type field effect transistors and CO gas sensors, Nanotechnology 20 (2009), 085203/1–085203/6.
[22] W.F. Zhang, Z.B. He, G.D. Yuan, J.S. Jie, L.B. Luo, X.J. Zhang, Z.H. Chen, C.S. Lee, W.J. Zhang, S.T. Lee, High performance, fully transparent and flexible zinc-doped indium oxide nanowire transistor, Appl. Phys. Lett. 94 (2009), 123103/1–123103/3.
[23] N. Singh, T. Zhang, P.S. Lee, The temperature-controlled growth of In_2O_3 nanowires, nanotowers and ultra-long layered nanorods, Nanotechnology 20 (2009), 195605/1–195605/7.
[24] W. Zhang, J. Jie, Z. He, S. Tao, X. Fan, Y. Zhou, G. Yuan, L. Luo, W. Zhang, C. Lee, S. Lee, Single zinc-doped indium oxide nanowire as driving transistor for organic light-emitting diode, Appl. Phys. Lett. 92 (2008), 153312/1–153312/3.
[25] S.Y. Li, C.Y. Lee, P. Lin, T.Y. Tseng, Low temperature synthesized Sn doped indium oxide nanowires, Nanotechnology 16 (2005) 451–457.
[26] M. Kumar, V.N. Singh, F. Singh, K.V. Lakshmi, B.R. Mehta, J.P. Singh, On the origin of photoluminescence in indium oxide octahedron structures, App. Phys. Lett. 92 (2008), 171907/1–171907/3.

Biographies

N. Singh completed his MTech (Materials Science) in 2007 from Indian Institute of Technology (IIT) Kharagpur, India. Currently he is pursuing his PhD in NTU Singapore. His research focus is on synthesis of oxide semiconductor nanowires for the application in chemical sensing.

C. Yan is currently pursuing his PhD in the Nanyang Technological University, Singapore. His research focus is on the synthesis of semiconducting nanowires.

P.S. Lee is an Associate Professor from the School of Materials Science and Engineering, Nanyang Technological University, Singapore. Her research interest is on the synthesis of nanowires and their applications.